Optical imaging through scattering media via magnetically modulated fluorescence

Nan Yang[1] and Adam E. Cohen[2,3,*]

[1]*School of Engineering and Applied Sciences, Harvard University, Cambridge, Massachusetts 02138, USA*
[2]*Department of Chemistry and Chemical Biology, Harvard University, 12 Oxford Street, Cambridge, Massachusetts 02138, USA*
[3]*Department of Physics, Harvard University, Cambridge, Massachusetts 02138, USA*
**cohen@chemistry.harvard.edu*

Abstract: A weak (< 1000 G) magnetic field can influence photochemical processes through its effect on electron spin dynamics in a photogenerated radical pair. In a solution of pyrene and dimethylaniline this effect manifests as magnetic field-dependent exciplex fluorescence. Here we describe magnetofluorescence imaging (MFI). A localized magnetic null defines a fluorescence detection volume, which is scanned through a sample to create an image. MFI forms an image without lenses and in the presence of arbitrarily strong optical scattering. The resolution of MFI is in principle not limited by optical diffraction, although the present implementation is far from the diffraction limit.

OCIS codes: (000.1570) Chemistry; (110.0113) Imaging through turbid media.

References and links

1. U. E. Steiner, and T. Ulrich, "Magnetic field effects in chemical kinetics and related phenomena," Chem. Rev. **89**(1), 51–147 (1989).
2. N. J. Turro, *Modern Molecular Photochemistry* (University Science Books, 1991).
3. S. Nagakura, H. Hayashi, and T. Azumi, *Dynamic Spin Chemistry: Magnetic Controls and Spin Dynamics of Chemical Reactions* (Wiley-Kodansha, 1998).
4. L. A. Margulis, I. V. Khudyakov, and V. A. Kuzmin, "Magnetic field effects on radical recombination in a cage and in the bulk of a viscous solvent," Chem. Phys. Lett. **119**(2-3), 244–250 (1985).
5. K. Bhattacharyya, and M. Chowdhury, "Environmental and magnetic field effects on exciplex and twisted charge transfer emission," Chem. Rev. **93**(1), 507–535 (1993).
6. H. J. Werner, H. Staerk, and A. Weller, "Solvent, isotope, and magnetic-field effects in geminate recombination of radical ion-pairs," J. Chem. Phys. **68**(5), 2419–2426 (1978).
7. N. K. Petrov, A. I. Shushin, and E. L. Frankevich, "Solvent effect on magnetic field modulation of exciplex fluorescence in polar solutions," Chem. Phys. Lett. **82**(2), 339–343 (1981).
8. H. J. Werner, Z. Schulten, and K. Schulten, "Theory of the magnetic field modulated geminate recombination of radical ion pairs in polar solvents: application to the pyrene–N, N-dimethylaniline system," J. Chem. Phys. **67**(2), 646 (1977).
9. D. N. Nath, and M. Chowdhury, "Effect of variation of dielectric constant on the magnetic field modulation of exciplex luminescence," Pramana **34**(1), 51–66 (1990).
10. C. R. Timmel, and K. B. Henbest, "A study of spin chemistry in weak magnetic fields," Philos. Transact. A Math. Phys. Eng. Sci. **362**(1825), 2573–2589 (2004).
11. K. Maeda, K. B. Henbest, F. Cintolesi, I. Kuprov, C. T. Rodgers, P. A. Liddell, D. Gust, C. R. Timmel, and P. J. Hore, "Chemical compass model of avian magnetoreception," Nature **453**(7193), 387–390 (2008).
12. H. Staerk, W. Kuhnle, R. Treichel, and A. Weller, "Magnetic field dependence of intramolecular exciplex formation in polymethylene-linked A-D systems," Chem. Phys. Lett. **118**(1), 19–24 (1985).
13. Y. Tanimoto, N. Okada, and M. Itoh Kaoru, "Magnetic field effects on the fluorescence of intramolecular electron-donor-acceptor systems," Chem. Phys. Lett. **136**(1), 42–46 (1987).
14. H. Cao, K. Miyata, T. Tamura, Y. Fujiwara, A. Katsuki, C. H. Tung, and Y. Tanimoto, "Effects of high magnetic field on the intramolecular exciplex fluorescence of chain-linked phenanthrene and dimethylaniline," J. Phys. Chem. A **101**(4), 407–411 (1997).
15. A. Weller, H. Staerk, and R. Treichel, "Magnetic-field effects on geminate radical-pair recombination," Faraday Discuss. Chem. Soc. **78**, 271–278 (1984).
16. Z. Yaqoob, D. Psaltis, M. S. Feld, and C. Yang, "Optical phase conjugation for turbidity suppression in biological samples," Nat. Photonics **2**(2), 110–115 (2008).

#131217 - $15.00 USD Received 7 Jul 2010; revised 25 Oct 2010; accepted 5 Nov 2010; published 22 Nov 2010

17. I. M. Vellekoop, and C. M. Aegerter, "Scattered light fluorescence microscopy: imaging through turbid layers," Opt. Lett. **35**(8), 1245–1247 (2010).
18. D. Huang, E. A. Swanson, C. P. Lin, J. S. Schuman, W. G. Stinson, W. Chang, M. R. Hee, T. Flotte, K. Gregory, C. A. Puliafito, and J. G. Fujimoto, "Optical coherence tomography," Science **254**(5035), 1178–1181 (1991).
19. H. F. Zhang, K. Maslov, G. Stoica, and L. V. Wang, "Functional photoacoustic microscopy for high-resolution and noninvasive in vivo imaging," Nat. Biotechnol. **24**(7), 848–851 (2006).

Magnetic field effects (MFE) in chemical reactions are a striking manifestation of quantum coherence under ambient conditions [1–3]. Magnetic field-dependent fluorescence occurs when the reaction product is a photon. Here we present magnetofluorescence imaging (MFI), in which an inhomogeneous magnetic field creates a localized fluorescence detection volume which is scanned through a sample to map the boundaries of the sample.

The interaction of ordinary magnetic fields (< 1000 G) with electron spins is far too weak to have any effect on chemical equilibria or thermally activated rates at room temperature. Nonetheless, in some photochemical reactions, weak magnetic fields (1-1000 G) change reaction rates by as much as 80% [4]. These surprising MFE arise because optical excitation generates a coherent spin state that is very far from thermal equilibrium. The spins evolve under the influence of local interactions and the external magnetic field. The final symmetry of the spin wavefunction—singlet or triplet—determines the allowed reaction pathway. MFE can occur when the reaction proceeds faster than the time for the spins to reach thermal equilibrium.

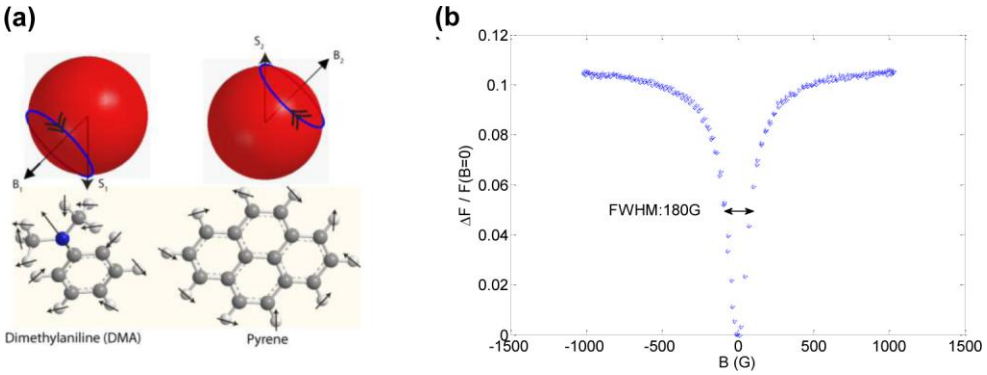

Fig. 1. Magnetic field effect on fluorescence of a solution of pyrene/dimethylaniline (DMA). (a) Top: Bloch spheres for two electron spins in the radical pair. Absorption of a photon induces electron transfer from DMA to pyrene, to generate a spin-correlated radical pair. The electrons start in a singlet state and each precesses around its local effective magnetic field, which has contributions from hyperfine interactions and an applied magnetic field. Bottom: schematic showing the magnetically active nuclei, each drawn as a classical magnetic dipole. The hyperfine fields combine to yield a random, approximately static effective magnetic field. (b) (Media 1) Fluorescence intensity as a function of external magnetic field. The MFE depends only on the magnitude of B, not its direction.

Several systems have been studied that show a MFE on fluorescence [5–7]. We employ a bimolecular system composed of an electron donor, dimethylaniline (DMA, 5×10^{-2} M), and an electron acceptor, pyrene (10^{-4} M). Werner and associates give a detailed theory of the MFE of this system [8]. Briefly, optical excitation induces electron transfer from DMA to pyrene to create a singlet radical pair. Each spin experiences hyperfine interactions with magnetically active nuclei in its vicinity. These random fields induce a singlet-triplet conversion, known as intersystem crossing (ISC). An external magnetic field partially decouples the electrons from the nuclei, slowing ISC and increasing the singlet state population. If the radicals later re-encounter, pairs in a singlet state may undergo electron back-transfer followed by exciplex fluorescence, while pairs in a triplet state cannot. Thus a magnetic field enhances the intensity of exciplex fluorescence.

#131217 - $15.00 USD Received 7 Jul 2010; revised 25 Oct 2010; accepted 5 Nov 2010; published 22 Nov 2010

The magnitude of the MFE is sensitive to the solvent properties, particularly the dielectric constant and viscosity [7,9]. We use a solvent of 3:1 tetrahydrofuran (THF):dimethylformamide (DMF) [9], which leads to an MFE of 10%, with a FWHM of 180 G. This MFE can be seen by eye as a small increase in fluorescence upon bringing a permanent magnet up to a vial of the solution under UV illumination (see Media 1). All chemicals were from Sigma Aldrich and used without further purification.

We reasoned that an inhomogeneous magnetic field would lead to a spatially varying rate of ISC, and thereby to a spatially varying fluorescence. In particular, a field with a localized null leads to a localized region in which ISC is faster—and the fluorescence lower—than in its surroundings. We scan this field null through a sample chamber containing a non-magnetic object immersed in a magnetofluorescent fluid. We record the total fluorescence intensity as a function of the location of the field null. The pattern of fluorescence intensity indicates the shape of the object. Due to the small fractional changes in fluorescence expected during the measurement, we dither the location of the magnetic null at a high frequency and use lock-in detection of the fluorescence.

Experimental apparatus

Figure 2(a) shows a diagram of the apparatus. Four permanent dipole magnets (K&J Magnetics DX0X0-N52) produce an octupole field in which $\mathbf{B} = 0$ along the entire z-axis. In the x-y plane, this arrangement creates a localized magnetic null at the origin. The magnets are cylinders with a diameter of 25.4 mm, a length of 25.4 mm, and a surface field of 6619 G. Opposing faces are 36 mm apart. Dithering coils are mounted concentrically with two of the magnets. Each coil is wound from 61 m of 18 gauge magnet wire. The inner and outer diameters are 4 cm and 8 cm, respectively. The coils are connected in series with a 4 μF capacitor for resonant driving. The octupole magnet and dithering coils are mounted on a Ludl precision scanning stage. The sample chamber, excitation and detection pathways are mounted to the optical table and do not move during the experiment. The magnet assembly is scanned relative to the sample.

The sample chamber is constructed from a ½" diameter black anodized aluminum tube (Thorlabs SM05L05) with top and bottom surfaces composed of optical windows (Anchor Optics AX45637). A size 12 Kalrez o-ring (VWR 14212-020) is placed between the windows to seal the fluid in the chamber and to set the separation of the windows to be 2 mm. The object to be imaged is immersed in a solution of pyrene/DMA contained in a sample chamber, which is mounted between the magnets. Ground glass windows (Edmund Optics NT62-616) are placed within the aluminum tube, 2 cm above and below the sample chamber. These windows scatter light strongly, and thereby prevent conventional optical imaging of the sample.

A 100 W mercury lamp with a 350 nm short pass filter (Asahi XUS0350) illuminates the top of the sample with 12 mW of UV light. The mercury line at 334 nm coincides with the absorption peak of pyrene. An emission filter (Chroma D435/90x) below the sample blocks transmitted excitation light and passes exciplex fluorescence to a 10 mm diameter acrylic light guide (Anchor optics AX27644), which carries the fluorescence to a photomultiplier tube (Hamamatsu H10492-013).

To acquire an image, the x-y translation stage moves the magnet assembly relative to the sample in a raster pattern, causing the dark spot to move across the sample (see Media 2). To enhance the signal-to-noise ratio we use a lock-in detection scheme. A function generator connects to an audio amplifier, which drives the dithering coils at 870 Hz and 1 A, r.m.s., corresponding to an AC field amplitude of 80 G at the magnetic null (see Media 3). Drive currents are chosen so the amplitude of the dithering is approximately half the width of the dark spot. The total fluorescence intensity develops a component at the modulation frequency only when the dithering carries the dark spot across the boundary of an object. The signal from the PMT is fed into a lock-in amplifier (Princeton Applied Research 5210), and the

#131217 - $15.00 USD Received 7 Jul 2010; revised 25 Oct 2010; accepted 5 Nov 2010; published 22 Nov 2010

signal driving the dithering magnets is used as a reference. We use a Labview program to control a data acquisition card (National instrument DAQ6259).

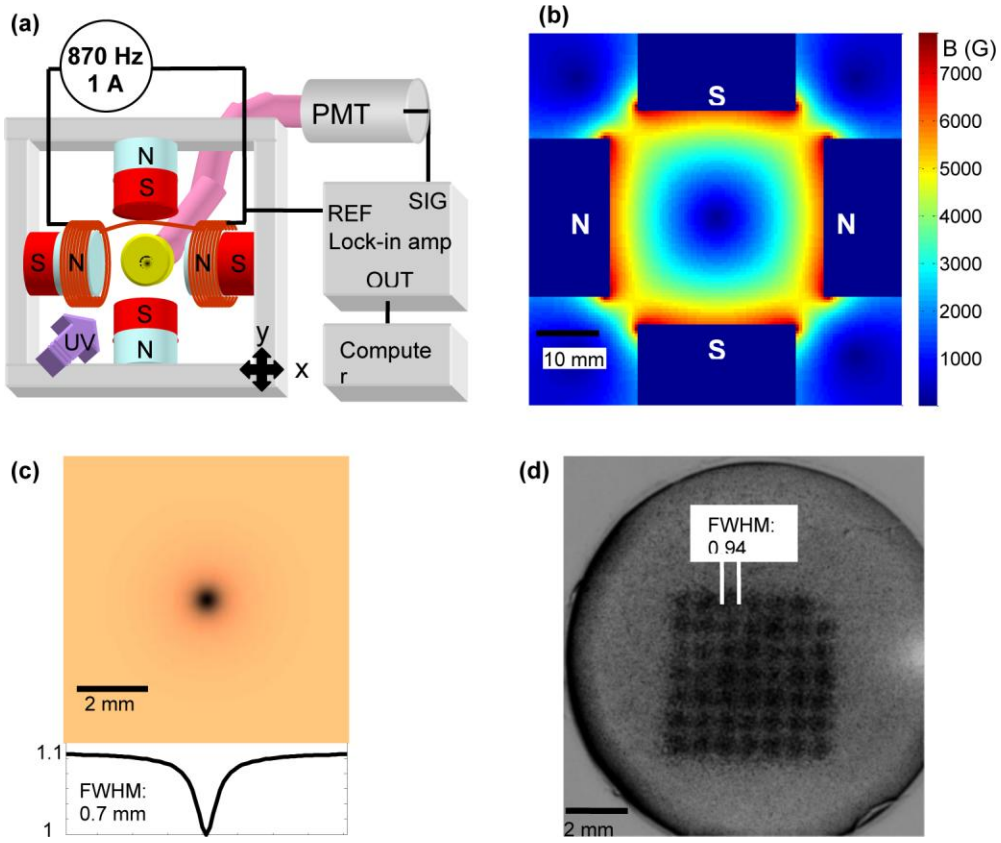

Fig. 2. Apparatus for magnetofluorescence imaging. (a) The sample is immersed in a solution of pyrene/DMA (yellow disk) and placed in an octupole magnet. UV illumination impinges from above and fluorescence is sent via 10 mm acrylic light guide to a photomultiplier (PMT). Bias coils dither the location of the magnetic null at 870 Hz for lock-in detection. A mechanical x-y stage scans the magnet assembly relative to the sample. (b) Simulation of the magnetic field strength due to the permanent magnets in the plane $z = 0$. (c) Predicted point spread function based on field profile from (b), and the MFE on fluorescence from Fig. 1(b). (d) (Media 2, Media 3) Direct optical imaging of the point spread function. The light guide and PMT were replaced by a CCD camera. The sample chamber was filled with pyrene/DMA and the exciplex fluorescence was imaged onto the camera. The octupole magnets were scanned across a 7 x 7 grid. The dark spots correspond to the locations of the null in the magnetic field. The point spread function has a FWHM of 0.94 mm.

We typically perform two x-y scans, with the sample rotated 90° about the z axis between each. The two outputs of the lock-in, acquired from corresponding points in the sample, are combined to associate a vector with each point. This vector points along the surface-normal of the object in the x-y plane.

We simulated the field of the permanent magnets by numerical integration of Maxwell's Equations in Matlab [Fig. 2(b)]. The field distribution was combined with the measured MFE for pyrene/DMA [Fig. 1(b)] to yield an estimated point spread function [Fig. 2(c)]. The result agrees well with the point spread function measured by acquiring a fluorescence image of the sample chamber containing only pyrene/DMA solution [Fig. 2(d)]. The dark spots in Fig. 2(d) indicate the locations of the null in the field as the magnets are moved relative to the sample.

#131217 - $15.00 USD Received 7 Jul 2010; revised 25 Oct 2010; accepted 5 Nov 2010; published 22 Nov 2010

The symmetry of the octupole arrangement ensures that the magnetic null exists along the entire *z*-axis. The point spread function broadens away from the plane $z = 0$, but this broadening is negligible over the 2mm vertical dimension of the sample chamber.

Results

MFI is insensitive to the path the light takes entering or exiting the sample, because the detection volume is determined entirely by the magnetic field. Thus one may acquire optical images in the presence of arbitrarily strong optical scattering. This property of MFI is dramatically demonstrated by imaging through our sample chamber, in which the only optical access is through ground glass plates. MFI penetrates the walls of the chamber, yielding the images shown in Fig. 3.

The samples imaged in Fig. 3 are made by cutting a 1 mm thick glass slide into strips. A dilute solution of sodium silicate is used to bind the strips together. We first acquire an MFI image of the sample chamber containing only a solution of pyrene/DMA. Then we acquire an image with the glass sample. The difference between these images shows the boundaries of the sample. By projecting the surface-normal vectors onto a single axis (45° from vertical, in this case), shadow images of the object are created. We emphasize that these images could not have been acquired by conventional imaging due to the strong scattering of light entering and exiting the sample.

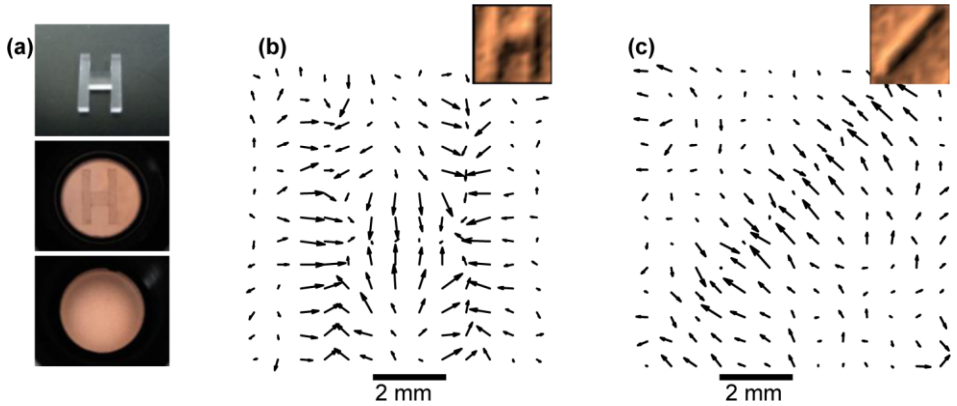

Fig. 3. Imaging through a scattering medium. (a) Sample cell. A glass object to be imaged (top) is placed in a chamber with a solution of pyrene/DMA (middle). The bottom and top of the chamber are blocked by ground glass plates so the object is obscured (bottom). (b) Magnetofluorescence images of the sample hidden inside the chamber. The vectors represent the local gradient of the MFE, which is only large at the solution / object interface. The quiver plot shows the boundaries of the object in (a). Inset: projected shadow image. (c) Quiver plot showing the boundaries of a single glass rod. Inset: projected shadow image.

Discussion

The spatial resolution of MFI is given by $\delta x = \sigma / \nabla B_0$, where σ is the width of the MFE (in G) and $\tilde{\nabla} B_0$ is the gradient in the field strength at the magnetic null (in G/mm). In our device, σ = 180 G and $\tilde{\nabla} B_0$ = 260 G/mm, leading to a theoretical resolution of 0.7 mm. Our experimentally determined resolution is 0.9 mm. Steeper gradients or narrower magnetic response curves lead to higher resolution. A steeper gradient is obtained by either increasing the strength of the octupole magnets, or by decreasing their size and separation. Material limitations determine the maximum strength of the octupole permanent magnets, so miniaturizing the octupole magnets provides the best route to higher field gradients. Strong permanent magnets may be fabricated down to the sub-micron scale, suggesting that the present system could be miniaturized by at least four orders of magnitude.

#131217 - $15.00 USD Received 7 Jul 2010; revised 25 Oct 2010; accepted 5 Nov 2010; published 22 Nov 2010

The number of resolvable spots along each axis is $N \approx \frac{L\nabla B_0}{2\sigma}$, where L is the distance between the pole pieces. The factor of 2 arises from the constraint that the sample must be no larger than $L/2$ along any dimension, to avoid collisions with the permanent magnets during scanning. Scaling the system to smaller size while keeping the magnetization fixed does not affect the number of resolvable spots because $L\tilde{N}B_0$ remains constant. The present system generates images with 13 x 13 resolvable points. To increase the number of resolvable points one must increase the sensitivity of the MFE.

Molecules with smaller hyperfine fields respond to smaller magnetic fields, and thus enable higher resolution imaging. Deuterated molecules have significantly reduced hyperfine fields and have been demonstrated to show greater sensitivity to magnetic fields [10]. Other electron donor/acceptor systems show magnetic sensitivity to fields as small as 0.4 G [11]. An outstanding chemical challenge is to design fluorescent systems with greater magnetic field sensitivity. Ideally such systems would also be photostable and water soluble.

A further challenge in MFI is to detect the small fluctuations in the fluorescence at the magnetic null, above the larger unmodulated fluorescence from the remainder of the sample. In our experiment, the maximum AC component of the PMT voltage is V_{AC} = 100 μV, while the DC background is V_{DC} = 500 mV. To achieve a shot noise-limited SNR of 10, one must acquire at least $n_{phot} = 100(V_{DC}/V_{AC})^2$ fluorescence photons at each pixel. This requirement can lead to unreasonably long image acquisition times. The background increases as $V_{DC} \propto N_{pix}$, where N_{pix} is the number of pixels, while the maximum AC signal is independent of N_{pix}. The acquisition time per pixel increases as N_{pix}^2, and the time per image increases as N_{pix}^3. Thus shot noise ultimately limits the number of pixels in an MFI image. To improve the signal-to-background ratio, one would like to increase the magnitude of the MFE. For our present system the MFE is about 10%. Attaching the donor and acceptor by a methylene chain dramatically increases the MFE, which reaches 47% for linked pyrene and DMA [12–14].

The signal-to-background ratio can also be improved by using a system in which the magnetic field *suppresses* fluorescence. For instance, the delayed fluorescence—in contrast to the prompt fluorescence used here—of pyrene/DMA is suppressed by a magnetic field [15]. Delayed fluorescence arises from radical pairs that undergo intersystem crossing into the triplet state. Electron back transfer leaves pyrene in an excited triplet state. When two triplet pyrenes collide, one pyrene can end up in an excited singlet state, which then emits delayed fluorescence. The timescale of delayed fluorescence is set by diffusional encounter of pairs of triplet pyrene, and is much longer than the prompt fluorescence lifetime of pyrene of ~100 ns. The intensity of delayed fluorescence is reduced by an external magnetic field.

We measured the MFE on delayed fluorescence of pyrene/DMA, using a pulsed N_2 laser for excitation and a gated avalanche photodiode for detection. A magnetic field reduces the delayed fluorescence by as much as 30% as shown in Fig. 4, suggesting that delayed fluorescence is a viable contrast mechanism for MFI. However, the delayed fluorescence is far more sensitive to ambient oxygen than is the prompt fluorescence, so the data must be acquired under rigorously degassed conditions. Delayed fluorescence is also far dimmer than prompt fluorescence, necessitating longer acquisition times. Finally, measurement of delayed fluorescence requires a pulsed or modulated light source, while prompt fluorescence can be measured with a regular mercury lamp. These factors significantly complicate the implementation of MFI with delayed fluorescence.

The ability of MFI to image inside scattering media may prove useful in biomedical imaging, as biological tissues scatter light strongly. Optical coherence tomography, photoacoustic microscopy, optical phase conjugation, and wavefront shaping allow imaging through scattering media, but these techniques have depth of penetration of 1 mm or less

#131217 - $15.00 USD Received 7 Jul 2010; revised 25 Oct 2010; accepted 5 Nov 2010; published 22 Nov 2010

[16–19]. MFI is in principle free from such limits, provided molecules with suitable fluorescence spectra and magnetic sensitivities are identified. Furthermore, MFI only senses magnetically sensitive fluorophores, and is thus insensitive to crosstalk from other fluorescent compounds. The spatial resolution of MFI is entirely independent of the strength of the optical scattering, provided that a sufficient number of fluorescence photons reach the detector. One can also conceive of applying MFI in a semi-infinite medium, in which case fluorescence would be detected in the backscattered direction rather than in the forward direction.

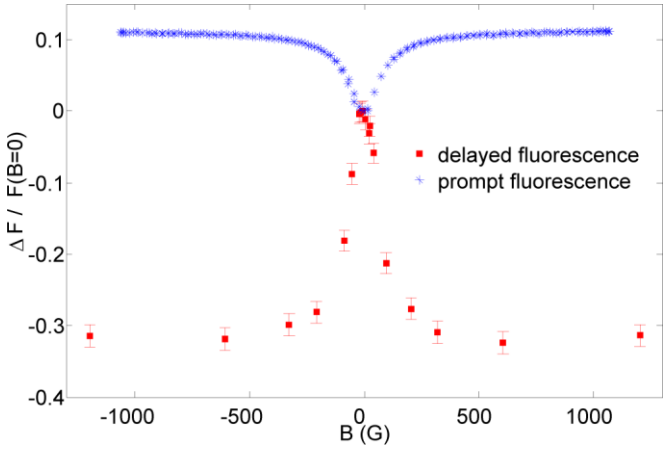

Fig. 4. MFE for prompt and delayed fluorescence of pyrene/DMA in degassed THF/DMSO (82%:18%). The uncertainties in the measurements are from photon shot noise. Error bars are shown for the delayed fluorescence measurements, and are negligible for the prompt fluorescence measurements.

Acknowledgements

This work was supported by the Defense Advanced Research Projects Agency (DARPA) YFA grant N66001-091-2104 and the Office of Naval Research (ONR) YIP grant N000140910868. N.Y. acknowledges the Natural Sciences and Engineering Research Council of Canada (NSERC) for funding his PGS D scholarship. Sample preparation was partially performed at the Harvard Faculty of Arts and Sciences (FAS) Center for Nanoscale Systems, a member of the National Nanotechnology Infrastructure Network, supported by the National Science Foundation (NSF) award ECS-0335765.